Structures and metamorphism at Brygfjell-Simafjell within the Rödingsfjället Nappe Complex, Nordland, Norway

BJØRGE BRATTLI

Brattli, B. 1996: Structures and metamorphism at Brygfjell-Simafjell within the Rödingsfjället Nappe Complex, Nordland, Norway. *Nor. geol. unders. Bull. 431*, 19-32.

Structures and metamorphic features are described from parts of the area of 1:50,000 map-sheet Korgen. The area investigated is situated within the Rödingsfjället Nappe Complex in the Caledonides of Nordland. The rocks are divided into two units, an upper unit named the Brygfjell Group consisting of a schist-marble complex, and an underlying unit, the Bjørnskolten Group, composed mainly of heterogeneous gneisses. The rocks have been affected by four phases (F_1, F_2, F_3 and F_4) of folding. The first deformation produced isoclinal folds with a penetrative schistosity, S_1. These structures are deformed by tight to near isoclinal F_2 folds, with NW-plunging axes and with near-horizontal axial planes. The F_2 folds control the large-scale outcrop pattern of the area. In appropriate rocks a poorly developed schistosity, S_2, is in places defined by the growth of white mica. The third deformation phase produced open synforms and antiforms of parallel type with vertical axial planes and WNW-ESE trending axes, while the fourth phase is represented by a gentle buckling of the rocks along N-S axes. Folds of the last two phases do not carry any axial planar cleavage or schistosity.

The metamorphic peak occurred during the first phase of folding, and is estimated to c. 680 °C and 7.5-8.5 kbar by use of the garnet-biotite thermometer, and observed reaction-isograds in different rocks. The highest garnet-biotite temperatures, which are in good agreement with the temperature interval for the observed reaction-isograds, are derived for garnet cores together with inclusions of biotite in the core areas. Calculations using garnet rims together with matrix biotite give temperatures which are about 100 °C lower than the maximum. It is proposed that this could represent the temperature conditions during the F_2 folding.

A second or retrograde mineral association is represented by the chloritisation of garnet, biotite and amphibole in appropriate rocks and a sericitisation/saussuritisation of plagioclase and Al-silicates. It is impossible to relate the secondary minerals to any specific structural elements. However, textural relationships indicate that the replacement processes have taken place over a long period of time, probably from pre-F_2 to post-F_4.

Bjørge Brattli, Department of Geology and Mineral Resources Engineering, Norwegian University of Science and Technology, 7034 Trondheim, Norway.

Introduction

The purpose of this investigation is to describe and quantify the metamorphism in part of the highest Caledonian nappe unit in Nordland and to propose a possible relationship between the metamorphic evolution and the structures. The study area is situated in the Rödingsfjället Nappe Complex (RNC) (Kulling 1955), c. 10 km north of the Bleikvassli sulphide mine in the mountains of Brygfjell-Tverrfjell- Sima-fjell. The RNC, together with the Helgeland Nappe Complex (HNC) (Ramberg 1967, Gustavson 1975), forms the Uppermost Allochthon of the north-central Caledonides. To the east the HNC/RNC is underlain by the Seve-Köli nappes (Fig. 1).

The Uppermost Allochthon is composed of medium- to high-grade and low-grade metasupracrustal rocks intruded by large massifs of gabbroic to granitic composition, (Gustavson 1975, 1978, 1982, Gjelle 1978, Tørudbakken & Brattli 1985, Brattli & Tørudbakken 1987, Gustavson & Gjelle 1991, 1992). The allochthon forms a large synformal structure between eastern and western antiformal culminations of Precambrian crystalline rocks (Fig. 1). During the Caledonian orogeny the Precambrian rocks were deformed together with the rocks of the Uppermost Allochthon. The individual nappe complexes have been divided into various tectonostratigraphical units and the boundaries between these units generally represent thrust contacts (Ramberg 1967, Stephens et al. 1985, Brattli & Tørudbakken 1987). The age and provenance of the Uppermost Allochthon is poorly known, but it is regarded as a major tectonic unit which has been transported a great distance. Riis & Ramberg (1979), Cribb (1981) and Brattli et al. (1982) have presented isotopic dating evidence that certain gneiss units within the RNC are of Precambrian age. The lower age limits of these rocks remain somewhat controversial. Skauli et al. (1992) have reported a metamorphic age of 464±22 Ma for the peak metamorphism at Bleikvassli. Age determinations of intrusive rocks in the RNC are sparse. Rb-Sr whole-rock age determination studies on foliation-discordant, granitic dykes near Umbukta in the RNC (Claesson 1979) indicate an age of 447±7 Ma. Farther north in the Beiarn Nappe Complex (BNC) (Rutland & Nicholson 1965), which is considered to be a sub-unit of the RNC, an age of 440 ±30 Ma has been reported on a post-tectonic (post the main fold episodes, F1 and F2) granite (Tørudbakken & Brattli 1985). Rb-Sr whole-rock age determinations on some gneisses (Harefjell gneisses) within the BNC have given ages of 415±26 and 470± 59 Ma (Cribb 1981). These rocks were previously interpreted by Rutland (1959) as metamorphosed supracrustals, but are now believed to be plutonic rocks (A.Solli pers.comm. 1996) which intru-

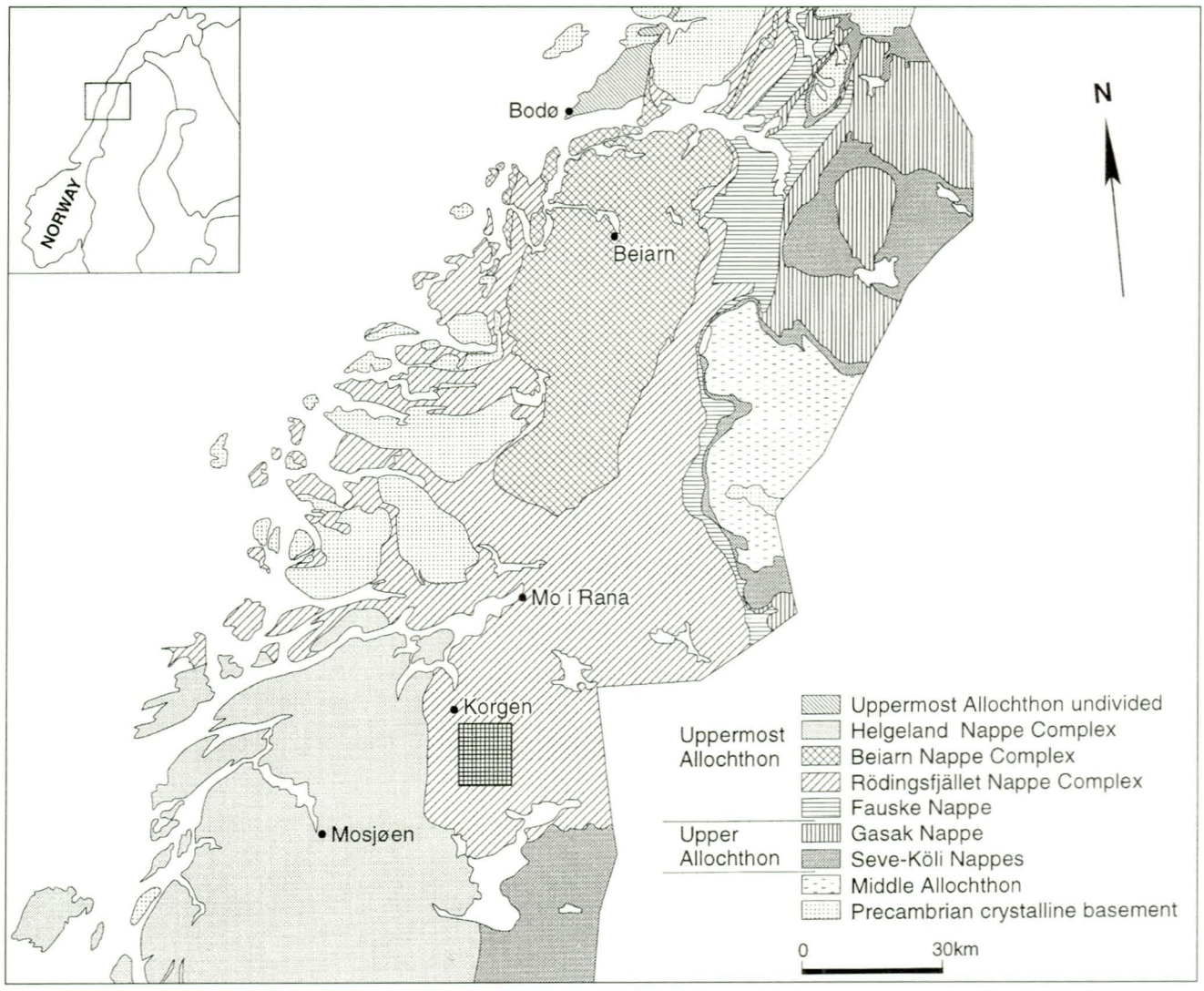

Fig. 1. Principal tectonostratigraphic units of parts of Nordland, north-central Norwegian Caledonides, based upon maps published by the Geological Survey of Norway (Norges geologiske undersøkelse). The shaded rectangle marks the area covered by this investigation.

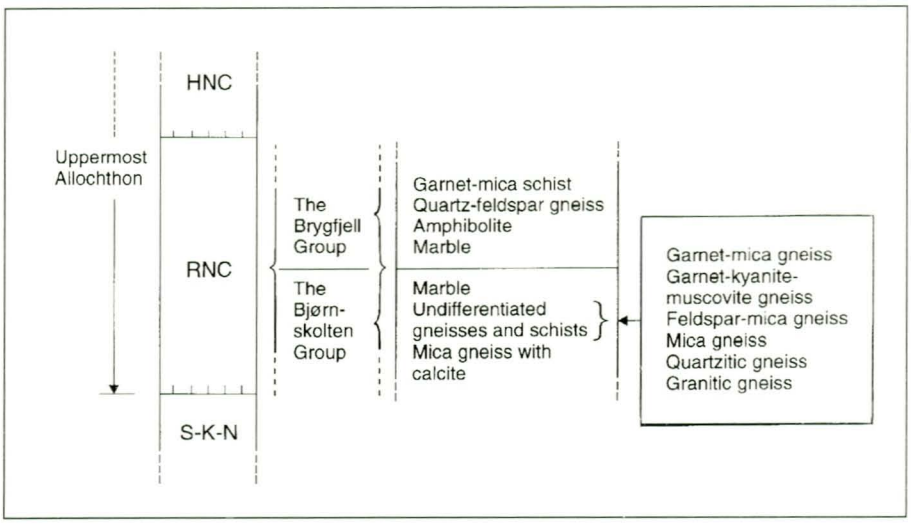

Fig. 2. Schematic tectonostratigraphic and lithostratigraphic succession for the investigated area. Abbrevations, HNC=Helgeland Nappe Complex, RNC=Rödingsfjället Nappe Complex, S-K-N=Seve-Köli Nappes

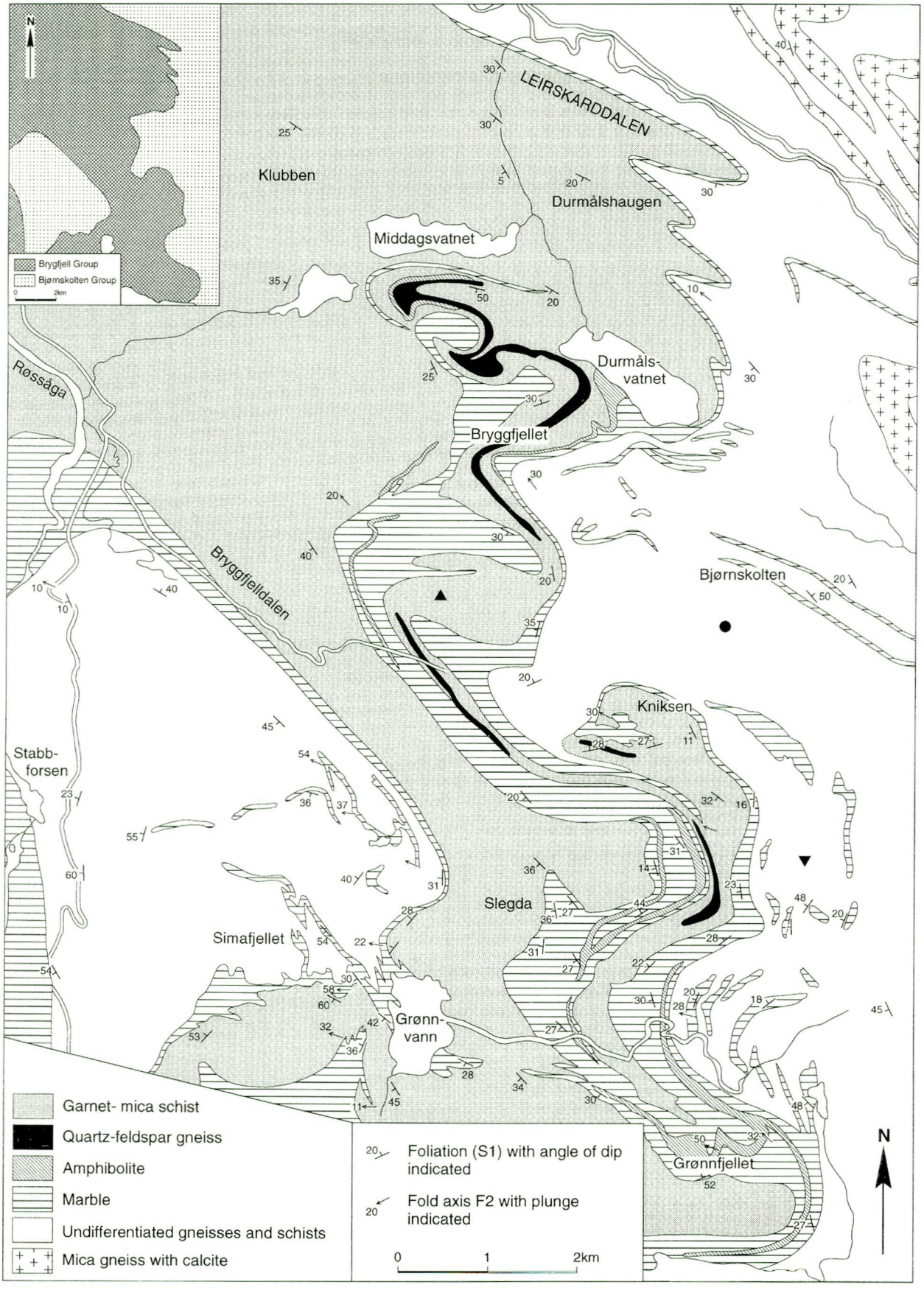

Fig. 3. Simplified geological map of the Brygfjell - Simafjell area within the Rödingfjället Nappe Complex, (see also Gustavson et al. 1990). Inset map in the top left corner shows the division into groups. The symbols mark the localities of the samples taken for the electron microprobe investigation (▲= sample 23.8, ▲= sample 13.8, ·=● sample 3.8).

ded between the F_1 and F_2 fold episodes. These ages, together with those from the RNC provide an upper limit for the main deformation and metamorphism in the Uppermost Allochthon of the Nordland Caledonides.

The investigated area covers a c. 200 km^2 region of the southernmost part of the 1:50,000 map- sheet Korgen (1927 II) and the northernmost part of the map-sheet Røsvatnet (1926 I). The rocks have been subdivided into two units. The upper unit is named the Brygfjell Group and consists of a schist-marble association, while the underlying unit, the Bjørnskolten Group, consists mainly of heterogeneous gneisses (Figs. 2 and 3). The Brygfjell Group can be correlated with the Anders Larsa Group in the Bleikvassli area (Ramberg 1967) while the Bjørnskolten Group is correlated with the Kongsfjellet Group in the same area. A simplified geological map is presented in Fig. 3. A preliminary version of the bedrock geology of map-sheet Korgen was published in 1990 (Gustavson et al. 1990).

In order to study the metamorphic conditions in the rocks, both index minerals (isograds) and mineral reactions (reaction-isograds) have been examined. A quantitative evaluation of the temperature and pressure conditions under the main metamorphism has been made by using the calibration for the partitioning of iron and magnesium between biotite and garnet in pelitic rocks, in combination with reaction-isograds for various mineral reactions.

Deformation

Studying the metamorphic history in an area requires a thorough integration with structural fieldwork as well as studies of microstructures in oriented samples. In the following section the different Caledonian structures are described, as they are observed in the field and under the microscope.

Folds

The rocks of the area are multiply deformed. Structures ascribed to four phases of folding (F_1, F_2, F_3, and F_4) have been found in both groups.

F_1 folds

Flattening seems to have been very intense during this deformation event, affecting the initially developed folds to ultimately produce isoclinal folds and a pronounced axial plane foliation, S_1. Thus, in many cases it is difficult to recognise F_1 folds. However, mapping of layers which act as markers has shown that it is possible to follow lithological layers around F_1 fold closures. At Slegda, a large F_1 fold has been recognised by mapping the amphibolites which constitute thin bands within the marble (Fig. 3). In many outcrops the layers seem to be parallel, but careful mapping has shown that they commonly represent the limbs of large-scale isoclinal F_1 folds. Despite a pronounced transposition of the hinge areas, defined by a penetrative preferred mineral orientation parallel to the axial plane of the F_1 fold, the layers can still be traced around the closures.

Fig. 4. Rootless intrafolial F_1 fold in mica schist. The figure illustrates how limbs become thinned and transposed into the plane of foliation.

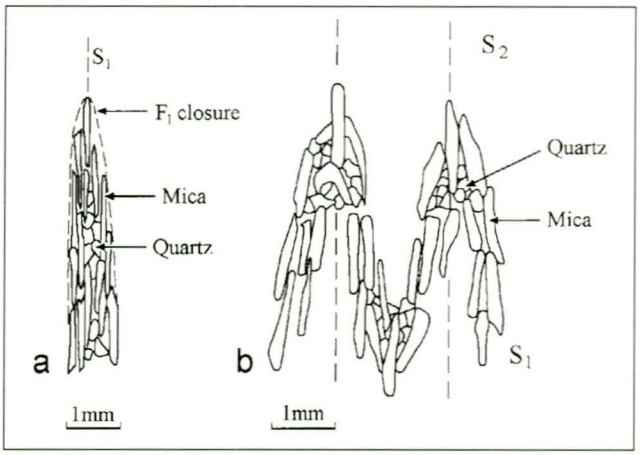

Fig. 5. Microscopic folds observed in thin-sections. (a) Parallel-oriented mica outlines a possible F_1 fold closure. Note that all minerals are parallel to the S_1 foliation. (b) F_2 folds in mica schist. Growth of white mica defines a poorly developed schistosity, S_2, in rocks of appropriate composition.

Mappable minor F_1 folds are seldom seen in outcrop. However, in rocks of appropriate composition, small bands and lenses (5-10 cm long) of quartz can be recognised as intrafolial and root-less intrafolial folds, indicating isoclinal folding. The limbs have become thinned and modified/transposed into the plane of foliation, ultimately causing the limbs to disappear (Fig. 4).

Clearly defined microscopic F_1 folds have not been observed, despite studies of thin-sections from different parts of large-scale F_1 structures. However, Fig. 5a illustrates how parallel-oriented mica may outline F_1 folds.

F_2 folds

The second fold episode is represented by large, recum-

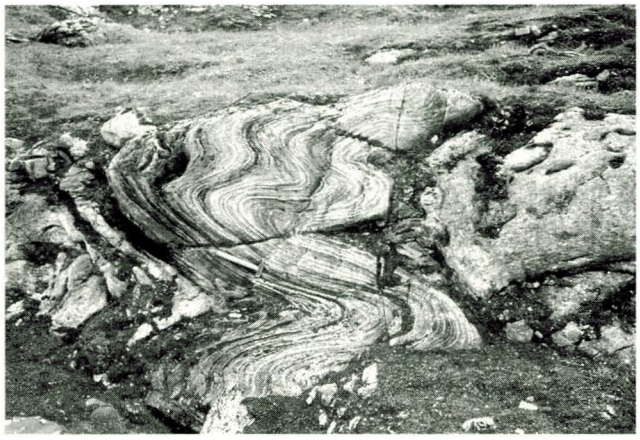

a)

b)

c)

Fig. 6. Different styles of F_2 folds developed as a consequence of the rock-types that are folded and the difference in rheology between the layers. (a) Class 1C folds. (b) Parallel folds. (c) Similar folds. The visual classification is based on Ramsay (1967).

bent, tight to isoclinal folds. The large-scale F_2 folds can easily be traced throughout the area, especially by following the marbles, but also by mapping the amphibolites and quartz-feldspar layers. The style of the F_2 structures is apparently quite variable (Fig. 3). However, this is mainly a consequence of the horizontal orientation of the axial planes. In areas where the axial planes cut the surface (topography) at right angles, as in the northern hillside of Grønnfjellet, the folds appear as close to tight structures. Otherwise, where the topography is smooth and the axial plane subparallel to the surface, the folds appear as close to open structures. The S_1 foliation is folded around the F_2 closures. Statistical distribution of the S_1 poles indicates that the mean axial direction of the F_2 folds plunges moderately towards WNW (Fig. 7a). This is in fairly good agreement with the most prevalent lineation orientation in the area.

Minor F_2 folds exposed in outcrop are very common. The fold style varies depending on the relationship to larger folds, the intensity of the deformation and the character of the alternating lithologies that are folded. F_2 minor folds are mainly tight to isoclinal. Some are clearly parasitic to larger folds with a long and a short limb. In rocks with alternating layers of mica schist and quartz-feldspar gneiss of equal thickness, the fold style is that of class 1C (Ramsay 1967) (Fig. 6a). In other areas where competent layers dominate, the folds appear as parallel folds (Fig. 6b). In cases with little or no competence difference between the layers, the folds are of a similar type (Fig. 6c). Measured fold axes plunge moderately (c. 20°) towards WNW and the axial planes dip gently (5-10°) between NW and WNW.

Microscopic F_2 folds have been observed in several thin-sections. Usually the minerals are folded around the F_2 closures. In some cases a second generation of white mica has been observed parallel to the axial plane of the F_2 folds (Fig. 5b). Quartz and epidote have also recrystallised in the hinge area of the folds.

F_3 folds

The F_3 folds are easily separated from the earlier structures on the basis of their style and the orientation of their axial planes. Usually they appear as parallel folds and form large, open synformal and antiformal structures. Plots of measured F_2 axial planes give a π_3 axis which plunges moderately (c. 20°) towards WNW (Fig. 7b). Because of interference between the synforms and antiforms and the topography (E-W oriented valleys), the folds may appear larger than they in fact are in reality.

Minor F_3 folds in outcrop have been observed in only a few places. The folds are open (120°), of parallel type and have symmetrical limbs (10-15 m long) and vertical axial planes.

F_4 folds

A gentle buckling of the rocks along N-S axes has produced open folds which are characterised by a small amplitude to wavelength ratio. The folds are only recognised in

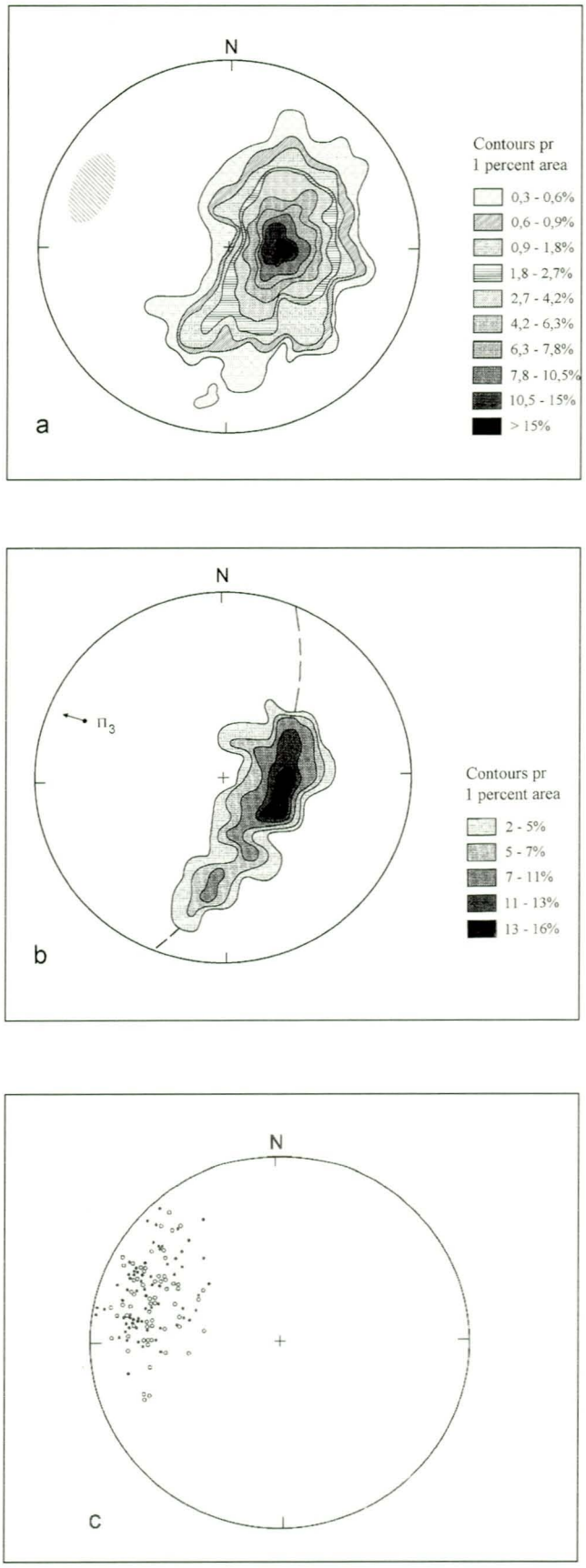

Fig. 7. Statistical representation of S and L measurements. Symbols used: — - = constructed π circle. (x = constructed fold axis. Stippled area represents F_2 and F_3 axes. o = F_2 fold axis. •= lineation. (a) Poles to 329 S_1 surfaces from the studied area. (b) Poles to 43 F_2 axial planes. (c) 63 fold axes and 68 unrelated lineations from the area.

areas with a smooth topography and where the rocks are very well exposed.

Planar structures

S_0/SS

In all units most of the rocks exhibit several types of planar structures. Genuine primary structures probably do not exist as the rocks have been modified and transformed by metamorphic and deformation processes. However, the lithological banding represented by alternating rock-types must be recognised as a primary feature, and is here abbreviated as S_0. In some rocks a planar structure defined by a layering is visible in hand specimen. In mica-rich rocks this can be described as a gneissic layering of alternating light and dark minerals, while in the marbles it is represented by an alternating grain-size distribution.These structures seem to be parallel to the lithological layering S_0, and are probably more a result of secondary transposition and metamorphic processes than a primary feature. In order to separate these from other planar structures, they have been designated SS.

S_1

The most prevalent and penetrative planar structure found throughout all units is the S_1 foliation. In mica-rich rocks it is defined by a domainal structure of lens-like and disc-like quartz and feldspar grains surrounded by a parallel arrangement of mica. In mafic rocks (amphibolite, calc-silicate rocks, etc.) it is defined by a parallel alignment of lamellar and prismatic chain silicates (amphiboles/pyroxene). The foliation is considered to be parallel or sub-parallel to the axial surface of the F_1 folds and hence to the S_0/SS structures, except in the hinge areas of the F_1 folds where the foliation intersects the lithological layering, S_0. In outcrop, however, all structures are aligned also in the fold closure area, because of the intense deformation and transposition during the F_1 folding episode (see above).

Altogether 329 S_1 poles have been plotted and contoured (Fig.7a). The contours do not define an unambiguous great circle and π_2 axis. Actually it is possible to draw many great circles through the contoured area. In doing so, the majority of the π axes fall within a restricted area (stippled) in the fourth quadrant. The poorly defined location for the π axis is presumably due to the fact that F_2 and F_3 axes are subparallel (see above) which has resulted in a broad spread of the S_1 poles. Thus, the stippled area represents both the F_2 and the F_3 axes.

In order to make a more precise decision on the location and orientation of the statistical F_3 axis, 43 F_2 axial planes have been plotted (Fig. 7b). The constructed π_3 axis plunges at 22 ° towards 290 °, which is within the stippled area for the π axes obtained from the S_1 poles (Fig. 7a).

S_2

Another schistosity, S_2, is observed in some samples. The

structure is poorly developed and rare in outcrop, but can be recognised in thin-section. Usually it is defined by the growth of white mica parallel to the axial planes of F_2 folds (Fig 5b). In appropriate rocks it may also be defined as an incipient crenulation cleavage in connection with the F_2 episode.

Lineations

In the studied area several types of linear structures have been observed. Only the most prevalent will be described here.

A fairly common (although not penetrative) linear structure is a mineral shape orientation. It is defined by a parallel alignment of grains with an elongate habit, like amphibole, and it is especially common in rocks containing such minerals. In most cases the lineation seems to be parallel to the F_2 fold axes. In the granitic gneiss at Simafjell another kind of mineral lineation is developed as a result of extreme elongation of feldspar. In some places the long axes of the elongated minerals (augen) have been measured to over one metre. This lineation is also oriented mainly parallel to the F_2 axial trend.

In rocks where an S_2 schistosity (see above) is developed, a lineation is also defined by the intersection line between S_2 and S_1.

In Fig. 7c, the measured linear structures (63 F_2 axis lineations and 68 unrelated linear structures) have been plotted. The stereographic presentation shows that the trend and plunge of the linear structures vary to a certain degree, but they mostly fall within the fourth quadrant of the stereogram. The spread is probably due to the fact that the lineations have been affected and 'disturbed' by later fold structures.

Petrography

In metamorphic rocks, characteristic minerals and mineral assemblages commonly provide a means of assessing the intensity and nature of the metamorphism and the relationship between the metamorphic history and the structures. The following section is concerned only with rocks and mineral assemblages which turned out to be of special interest for the evaluation of the metamorphic conditions. Other rock-types will not be described in this context. The nomenclature is based on quantitative mineralogical composition, and is after Winkler (1979).

Pelitic rocks (metapelites)

The metapelitic rocks are dominated by mica schists and mica gneisses. Based on field studies and modal analyses (fifteen samples), it is possible to separate between several types of schists/gneisses where the most important in this connection are; garnet-mica schist (most common in the Brygfjell Group, see Figs. 2 and 3), garnet-mica gneiss and garnet-kyanite-muscovite gneiss (restricted to the Bjørnskolten Group, see Figs. 2 and 3). All samples contain quartz, plagioclase, biotite, white mica, epidote/clinozoisite and garnet. Kyanite may appear in the garnet-mica schist, but is more common in the garnet-mica gneiss where it makes up to 5 % of the mode (in certain narrow zones in the garnet-kyanite-muscovite gneiss it makes up as much as 30%). Staurolite is present in the gneisses as inclusions in garnet together with quartz, biotite and white mica, but has never been observed in the matrix. Calcite has been found in only two samples of the garnet-mica schist. Chlorite is rather rare, but is recognised in a few samples as an alteration product after garnet and biotite. The mineral occurs either along grain boundaries or cracks (garnet). In biotite it may be present as 'sandwich' layers coherently disposed between relict layers of biotite. The mineral assemblages in the different rocks are summarised below.

Garnet-mica schist: Qz + $Pl_{An\ 36—40(core)}$ + Bt + Ms + Ep/Czo + Gt ± Ky ± Cal ± Chl
Garnet-mica gneiss: Qz + $Pl_{An\ 36(core)}$ + Bt + Ms + Ep/Czo + Gt + Ky ± St ± Hbl ± Chl
Garnet-kyanite-muscovite gneiss: Qz + Pl + Ky + Ms + Gt ± Bt ± St ± Chl

Amphibolite

Plagioclase and hornblende make up the bulk mineralogy of the amphibolites. All other minerals are modally subordinate. The mineral assemblage, based on studies of five thin-sections, is listed below. Epidote may appear in small amounts (< l%), but mostly it is lacking.

Amphibolite: Hbl + $Pl_{An\ 32\text{-}36(core)}$ + Bt + Qz ± Gt (± Ep) ± Chl

Siliceous carbonate rocks

Impure (siliceous) limestones/dolomites exist as a transition zone along the border between the marbles and the metapelites. Rocks consisting of quartz, dolomite and either calcite or magnesite remain unaffected at very low-grade metamorphism. At higher temperatures some minerals start to react and at high grade numerous reactions occur between the minerals. Based on thin-section studies (8 samples), it is possible to separate between three types of mineral associations (reactions).

Dolomitic limestone, (type A): Tlc + Cal + Tr + Dol
Siliceous dolomitic marble, (type B): Tr + Cal + Dol + Qz
Siliceous dolomitic marble, (type C): Tr + Di + Cal + Dol + Qz.

Relation between mineral growth and structures

It is possible to distinguish between two stages of mineral growth. The main mineral assemblage defines the S1 foliation. In the metapelites S_1 is outlined by minerals such as kyanite, biotite, garnet, muscovite, plagioclase and quartz, while in the amphibolites the foliation is defined by hornblende, plagioclase, biotite and in some cases garnet. In the siliceous carbonate rock the textural features are not so well developed as in the metapelites. However, the mineral associations (types A, B and C) listed above are considered to be syntectonic, i.e. they have had their principal growth period in connection with the main fold episode, probably during the formation of the penetrative planar foliation.

The main mineral assemblages are usually folded around microscopic F_2 folds. However, some minerals may show a zonation where the outermost rims cut the foliation. One such mineral is garnet. In metapelites and amphibolites the garnets have inclusion-rich cores (see above), in some cases with snowball structure (S_i), followed by massive idioblastic rims. The S_i seems to be parallel with the S_1 (or S_e), indicating that the main growth must have been syntectonic with respect to F_1. The rims usually cut the main foliation S_1, and must therefore be post-tectonic to F_1. In appropriate rocks a later phase of white mica is partly wrapped around and has partly grown into the rims of the garnet. This mica (which must be separated from the randomly distributed muscovite, see below) probably belongs in time to the muscovite which appears to grow parallel to the S_2 schistosity, indicating that the rims are partly pre-tectonic to F_2 and partly post-tectonic to F_2.

Other minerals which are zoned are plagioclase and epidote. Plagioclase typically exists with a gradual zonation ranging from andesine (An_{36-40}) in the cores to oligoclase (An_{26-30}) in the rims. The plagioclase is usually sericitised/saussuritised, especially in the cores. Together with quartz, the mineral forms lenses and bands (particularly in the gneisses) parallel to the S_1. It is reasonable to assume that the plagioclase core is in equilibrium with the main mineral assemblage defining the S_1 foliation, while the rim is in equilibrium with the later formed retrograde mineral assemblage (see below). Epidote appears as idiomorphic grains, with interference colour ranging from third order (cores) to low second order and even middle first order (rims). The opposite zonation has also been observed. Epidote may also occur as needles in connection with the saussuritisation of the plagioclase (this phase should be separated in time from the idiomorphic grains in the matrix). The epidote is randomly distributed relative to the main foliation, S_1, but at least some of the grains seem to be folded around microscopic F_2 folds. The growth must therefore have taken place over a long period of time, probably from post-F_1 to post-F_2 and maybe even into the F_3 phase (see below).

Except for a local redistribution of quartz located in the hinge areas of the F_2 folds and the presence of white mica parallel to the axial plane of the F_2 folds, there is no specific mineral growth which can clearly be asccribed to the F_2 deformation. The minerals formed during the F_1 deformation were, with small modification (zoned minerals), also stable under the F_2 deformation. The zonation indicates that the growth has probably taken place under varying PT conditions within the regional metamorphic belt. However, as most of the minerals belonging to the assemblage actually define the main foliation, S_1, their principal growth period must have been during the F_1 deformation.

The second or retrograde mineral association is represented by chloritisation of garnet, biotite and amphibole in appropriate rocks and a sericitisation/saussuritisation of plagioclase and Al-silicates. Randomly distributed muscovite and epidote also probably belong to the retrograde assemblage.

The replacement processes have probably taken place over a long period of time involving many reactions and various stages of alteration. It is impossible to relate the secondary or retrograde mineral assemblages specifically to any one of the structural elements. However, as the chloritisation has affected the massive idioblastic rims of the garnet, the process must have taken place after the formation of the rims, and therefore after the F_2 phase.

Metamorphic conditions

The investigated metapelites present several interesting mineral relationships that need to be discussed. Kyanite is the stable aluminosilicate in the rocks. It is found as a matrix mineral, usually parallel or sub-parallel to the S_1 foliation. The occurrence of the mineral indicates that the pressure and temperature are above or along the ky-line (Fig. 9) The most important mineral association is found in the garnet-kyanite-muscovite gneiss, represented by the occurrence of staurolite, quartz, kyanite and garnet. According to Winkler (1979) staurolite starts to decompose in quartz-bearing rocks at about 670 °C. The 'coexistence' of the minerals has therefore been extensively studied in thin-section. It is important to note that staurolite is found only as inclusions in garnet together with quartz and never as a matrix mineral. Kyanite, however, is the dominant alumino-silicate in the matrix and is also present as very small inclusions, together with staurolite and quartz, in the garnet. These observations lead to the conclusion that there must be at least two local medium-grade sub-assemblages in the rocks; one sealed in the garnet and probably represented by the equilibrium reaction (Bucher & Frey 1994, p. 202):

(1) staurolite + quartz = almandine garnet + kyanite + H_2O

and one in the matrix represented by the coexistence of garnet and kyanite.

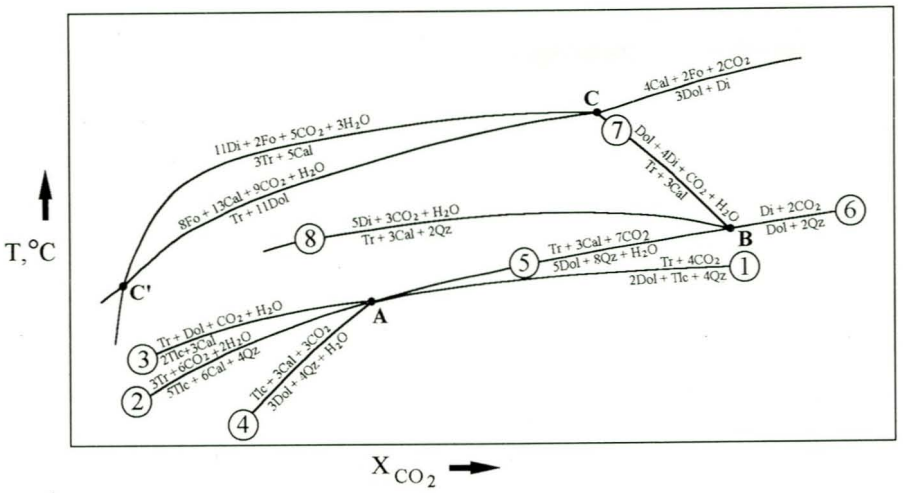

Fig. 8. Schematic TX_{CO2} diagram showing important equilibria and invariant points in the siliceous carbonate system (after Eggert & Kerrick 1981). Abbreviations: Cal = calcite, Di = diopside, Dol = dolomite, Fo = forsterite, Qz = quartz, Tlc = talk, Tr = tremolite.

The equation (1) defines a line in a PT diagram (Fig. 9). In the quartz-saturated matrix all staurolite is replaced by garnet and kyanite (see eq. 1). The two-mineral assemblage (Grt (alm) + Ky) is diagnostic for the initial stages of upper amphibolite facies.

In the amphibolites the main mineral assemblage consists of andesine, green hornblende, biotite ± garnet. This is a typical amphibolite-facies association, stable at a temperature around 600°C. According to Bucher & Frey (1994) clinopyroxene appears at higher temperatures, with the diopside-hedenbergite series as the dominant cpx at around 650°C. In this case no such minerals have been observed.

The mineral association in the siliceous carbonate rocks also exhibits some very interesting relationships. Most of the minerals have taken part in one or more reactions. Based on thin-section studies, the following transformations between the minerals are observed:

In type A: Reaction between tremolite, dolomite, calcite and talc
In type B: Dolomite ☞ tremolite
In type C: Tremolite ☞ diopside

Comments on reaction A
The most usual association is tremolite, dolomite, talc and small amounts of calcite. Quartz is not observed in connection with this association. In cases where calcite is in contact with tremolite, the latter appears with a rim of newly formed dolomite. A possible formation sequence could be after the following equations (Winkler 1979); see also Fig. 8:

(2) 5 Tlc + 6 Cal + 4 Qz = 3 Tr + 6 CO_2 + 2H_2O
(3) 2 Tlc + 3 Cal = Tr + Dol + CO_2 + H_2O

At the time when all quartz has been consumed, talc, calcite and tremolite are the stable minerals (eq.2). At slightly higher temperatures, talc and calcite will react to form more tremolite and dolomite (eq.3). The reactions may explain why quartz is apparently lacking and why tremolite is present with a rim of dolomite.

In order to facilitate the equilibrium reactions, the rocks must contain talc. The mineral is stable over a wide range of physical conditions (P,T, XCO_2) and could be formed as a result of an early reaction between dolomite and quartz (Winkler 1979); see also Fig. 8:

(4) 3 Dol + 4 Qz + H_2O = Tlc + 3 Cal + 3 CO_2

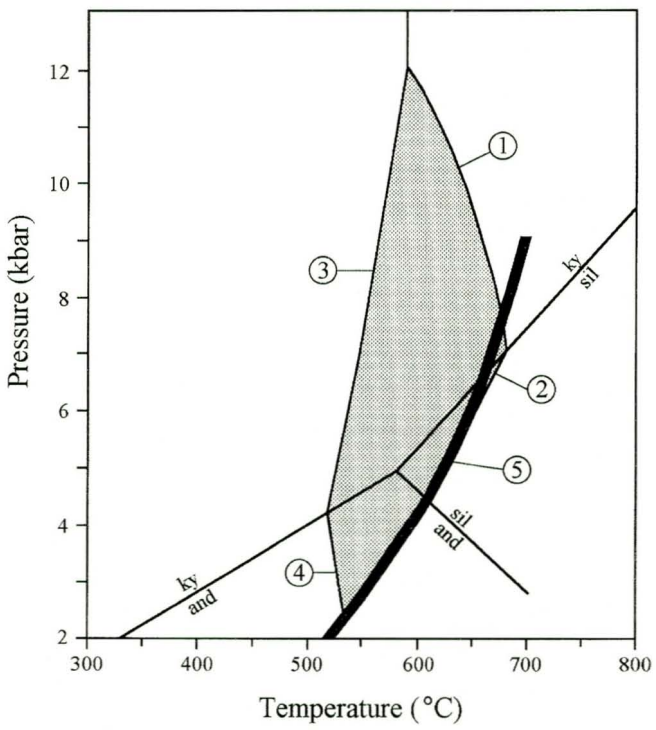

Fig. 9. PT-diagram showing some important equilibrium reactions. Shaded field: coexistence of staurolite + quartz. (1) 75 St + 312 Qz = 100 Alm + 575 Ky + 150 H_2O. (2) 75 St + 312 Qz = 100 Alm + 575 Sil + 150 H_2O. (3) 8 Cld + 10 Ky = 2 St + 3 Qz + 4 H_2O. (4) 8 Cld + 10 And = 2 St + 3 Qz + 4 H_2O. (5) Constructed curve based on the position of the invariant assemblage (B) (siliceous limestone) at 2, 4, 6, 8 kbar (see also Eggert & Kerrick 1981). The positions of reactions (1), (2), (3), (4) are after Bucher & Frey (1994).

The conclusion must be that in dolomite limestone of type A, there exists a local equilibrium assemblage represented by equation (3) and observed in thin-section as an association of Tlc + Cal + Tr + Dol. Lack of quartz and an 'unfavourable' mole fraction of XCO_2 are probably the controlling factors preventing the formation of diopside (Fig. 8).

Comments on reaction B

The principal mineral association consists of quartz, tremolite, calcite and dolomite. Studies of thin-sections show that tremolite is growing from dolomite as this decomposes. As calcite also seems to form in connection with the replacement of dolomite, the following reaction is proposed (Winkler 1979); see also Fig. 8:

(5) 5 Dol + 8 Qz + H_2O = Tr + 3Cal + 7 CO_2

The equilibrium equation represents a prograde evolution which will continue to produce tremolite as the temperature increases. This is a typical middle amphibolite-facies associations which represents temperatures and pressures of c. 600 °C and 5-6 kbar (Bucher & Frey 1994).

Comments on reaction C

In this type of rock, diopside makes up as much as 60 modal % and constitutes the main mineral. Depending on the existing reactants in the rock and the physical conditions (T, XCO_2), the formation of diopside may take place after the following reactions (Winkler 1979); see also Fig.8.

(6) Dol + 2 Qz = Di + 2CO_2
(7) Tr + 3 Cal = Dol + 4 Di + CO_2 + H_2O
(8) Tr + 3 Cal + 2Qz = 5Di + 3 CO_2 + H_2O
(9) From the reaction in the invariant point B: Qz + Tr + Di + Dol + Cal

Studies of thin-sections have shown that all the minerals in reaction (9) are present, which indicates that the rock has reached the invariant point B, probably along reaction (5) in Fig. 8. Formation of diopside according to reactions (6), (7) or (8) is not possible as long as the invariant mineral assemblage is present. As an example, diopside forms from reaction (8) only if reaction (5) (see above) has consumed all quartz at some lower temperatures, which is not true in this case.

In a study of dolomitic limestone carried out by Eggert & Kerrick (1981), the temperature interval for the equilibrium reactions and the position of the invariant points have been established as a function of p_{fluid} and XCO_2. According to the experimental calibrations, it is possible to construct curves for minimum and maximum conditions of XCO_2. Of all the possible equilibrium reactions above, reaction (9) reflects the highest temperature and is therefore the most interesting in this connection. Based on the position of the invariant point B at 2, 4, 6 and 8 kbar (see Fig. 8 in Eggert & Kerrick 1981), a curve has been constructed (line 5 in Fig. 9). Because of some uncertainties in the locations of the invariant points, the curve defines a broad line in the pT-diagram. However, using the information from the limestone in combination with the information from the garnet-kyanite-mica gneiss, it is possible to conclude that the temperature and pressure must have been equal to or greater than c. 675 °C and 7.7-7.9 kbar (the PT estimate is based on the intersection point between line 5 and line 1 in Fig. 9).

Geothermobarometry

In order to make the determination of the maximum PT conditions as precise as possible, a geothermobarometric study has been carried out on biotite and garnet and combined with the results from the petrographic investigation.

Using thermobarometry to determine the temperature and pressure at which the rock was metamorphosed is based on the assumption that the minerals are formed at equilibrium. However, it is questionable whether or not the minerals in a rock ever achieved equilibrium. According to Winkler (1979), it is possible to find different generations of sub-assemblages in a rock, hopefully each in a state of local equilibrium. The succeeding work is based on these assumptions.

Analytical methods and procedures

The most widely used geothermometers for metamorphic rocks involve the exchange of Fe^{2+} and Mg in the following minerals; olivine, garnet, clinopyroxene, orthopyroxene, biotite, phengite, chlorite and hornblende. The composition of the rocks (or the presence of minerals) will therefore place restrictions on the type of thermometer that can be used. In this particular case, garnet and biotite are common minerals in the metapelites. When the minerals are in mutual contact, it is anticipated that they are in equilibrium and can be used as a thermometer. The garnet-biotite exchange thermometer exists in many versions and it is used in a wide variety of rocks and over a broad range of metamorphic conditions. However, because of insufficient knowledge of how impurities affect the Fe^{2+}-Mg exchange between the minerals (see, for instance, Bhattacharya et al. 1992 and Spear 1993) it is difficult to choose between the many versions. For that reason the Ferry & Spear (1978) original thermometer is used in this work.

$$T\,(°C) = (2089 + 9.56\,P\,(kbar))/(0.782 - \ln K_D) - 273$$

The authors suggested that the thermometer should be restricted to usage for garnets low in Ca and Mn, with (Ca + Mn)/(Ca + Mn + Fe + Mg) ≤ 0.2 and with biotites low in Al^{vi} and Ti, with (Al^{vi} + Mn)/ (Al^{vi} + Ti + Fe + Mg) ≤ 0.15.

As the K_D values will vary as a function of inhomoge-

neities and zonation effects in the minerals; it is important to have a strategy for selecting the 'right' K_D values. One way is to choose the analyses which provide the lowest K_D values ('the K_D-min. method'). This method will give the highest temperature and hence information about the metamorphic peak. In order to be reasonably sure that the selected K_D value really represents the highest temperature, the choice must be based on a number of analyses. An interesting aspect of the 'K_D-min. method' is that if the same philosophy is used for the highest K_D value ('K_D- max. method'), this should provide information about the lowest equilibrium temperature for the coexisting minerals.

The metapelites in the investigated area contain poikiloblastic garnet with inclusions of mica, quartz and in some cases staurolite. The mica is mainly muscovite, but biotite may also occur. The garnet is usually represented by an outer idioblastic rim which, in contrast to the core, is mostly free of inclusions. The rim seems partly to cut the main biotite schistosity. In order to infer a possible metamorphic evolution over time, the poikiloblastic garnets (with the rims) were chosen for the analysis. It should also be stressed that the minerals (garnet and biotite) should look as fresh as possible (no sign of retrograde chlorite associated with the grains). It was decided to concentrate the microprobe analyses on two types of mineral relationship:

1. Core-areas of garnet together with inclusions of biotite located within that area (the biotite inclusions are very small).

2. Outermost inclusion-free rim of the garnet together with biotite in the matrix in contact with the rim.

After thin-section studies (30 samples from the metapelites in the area), three different rock samples, two from the garnet-mica schist/gneiss and one from the garnet-kyanite-muscovite gneiss, were chosen for the investigation (Fig 3). The selected samples all displayed the 'desired' biotite-garnet association described above. In each sample several garnet-biotite associations were analysed. Altogether, 12 pairs of garnet (core composition)-inclusion biotite and 16 coexisting pairs of garnet (rim composition)-matrix biotite were analysed according to the following procedure. In analysing the biotite in the matrix the electron beam was directed towards the border zone of the grains which were in contact with the rim of the garnet. In calculating the K_D values, all iron in the biotite is initially regarded to be in the ferrous state. Examples of electron microprobe analyses are given in Tables 1 and 2.

Results and discussions

It seems to be possible to differentiate between two 'populations' or groups of K_D values; one with 'low' K_D values represented by the garnet-core area + inclusions

Table 1. Examples of electron probe microanalyses of garnet.

Sample	1.3, 13.8 rim	1.4, 13.8 rim	3.6, 23.8 rim	1.5, 3.8 core	3.2, 23.8 core	2.6, 3.8 core
SiO_2	38.40	38.57	40.05	35.87	40.12	36.62
TiO_2	0.01	–	0.28	–	–	0.07
Al_2O_3	21.77	21.73	22.38	21.23	22.22	22.56
Fe_2O_3	31.45	31.28	29.33	29.42	28.86	29.22
MnO	0.38	0.53	1.27	1.01	1.90	1.90
MgO	4.92	4.77	5.35	5.35	5.39	5.21
CaO	5.84	5.81	6.19	5.42	6.19	6.16
Na_2O	–	–	0.05	–	0.03	0.08
K_2O	–	–	–	–	–	–
Total	102.83	102.71	104.96	98.34	104.74	101.82
Formula (based on 12 oxygens)						
Si	2.952	2.968	3.001	2.869	3.009	3.250
Al^{IV}	0.048	0.032	–	0.131	–	–
Ti	0.001	–	0.013	–	–	0.005
Al^{VI}	1.919	1.934	1.971	1.865	1.963	1.170
Fe^{3+}	0.128	0.166	0.014	0.266	0.030	0.332
Fe^{2+}	1.885	1.842	1.822	1.696	1.776	1.818
Mn	0.023	0.032	0.081	0.067	0.117	0.140
Mg	0.566	0.544	0.594	0.638	0.603	0.688
Ca	0.479	0.480	0.495	0.465	0.495	0.586
Na	–	–	0.007	–	0.005	0.005
K	–	–	–	–	–	–
Total	8.000	8.000	8.000	8.000	8.000	8.000
$\frac{Ca+Mn}{Ca+Mn+Fe+Mg}$	0.19	0.16	0.19	0.20	0.20	0.20

Table 2. Examples of electron probe microanalyses of biotite.

Sample	1.10, 13.8 matrix	1.2, 13.8 matrix	3.4, 23.8 matrix	1.1, 3.8 inclusion	3.3, 23.8 inclusion	1.9, 3.8 inclusion
SiO_2	39.48	37.16	38.67	38.69	38.75	37.76
TiO_2	1.62	1.80	1.53	1.57	1.96	1.42
Al_2O_3	18.17	18.36	18.40	17.73	18.65	17.96
Fe_2O_3	15.50	16.83	16.42	16.10	16.08	15.87
MnO	0.02	0.03	–	–	–	–
MgO	13.04	13.30	13.29	13.37	13.36	13.21
CaO	–	–	–	–	–	–
Na_2O	0.25	0.31	0.20	0.23	0.42	0.39
K_2O	8.30	9.00	9.28	9.12	9.44	8.42
Total	96.40	96.87	67.82	96.87	98.70	95.07
Formula (based on 22 oxygens)						
Si	5.744	5.470	5.613	5.657	5.569	5.611
Al^{IV}	2.256	2.530	2.387	2.343	2.431	2.389
Ti	0.175	0.194	0.165	0.175	0.207	0.159
Al^{VI}	0.851	0.650	0.746	0.709	0.729	0.716
Fe	1.877	2.060	1.984	1.964	1.934	1.962
Mn	0.003	0.003	–	–	–	–
Mg	2.819	2.916	2.871	2.903	2.857	2.975
Ca	–	–	–	–	–	–
Na	0.070	0.088	0.052	0.070	0.104	0.107
K	1.536	1.696	1.723	1.702	1.726	1.605
Total	15.273	15.607	15.541	15.522	15.557	15.474
$\frac{Al^{VI} + Mn}{Al^{VI}+Mn+Fe+Mg}$	0.17	0.15	0.13	0.15	0.16	0.15

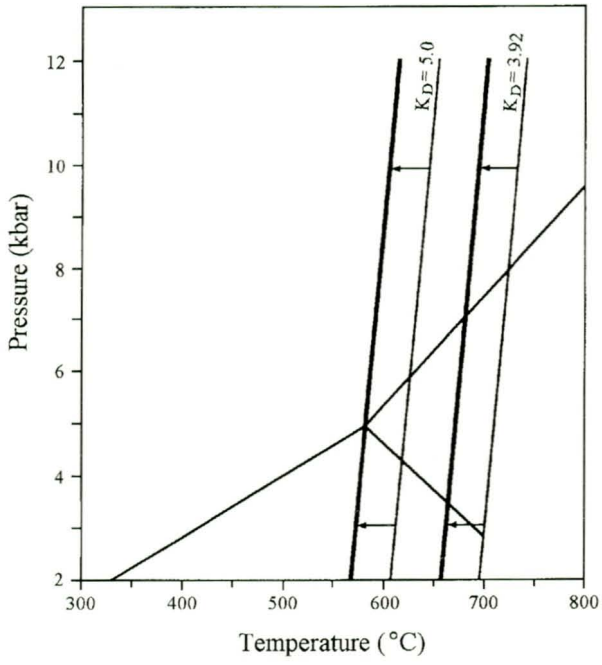

Fig. 10. K_D lines using the garnet-biotite calibration of Ferry & Spear (1978). The lowest K_D values are from the garnet cores together with inclusions of biotite in the garnet core area. The highest K_D values are from the garnet rims together with matrix biotite in contact with the garnet. The thick lines show the positions in the PT diagram after adjusting for ferric iron in the biotite (see text).

of biotite, and one with 'high' K_D values represented by the garnet-rim + matrix biotite. The K_D values from the first group vary between 4.35 and 3.92, while those from the second group range from 5.0 to 4.43. Using the 'K_D min. method' on the low-value group and the 'K_D -max. method' on the high-value group gives a maximum temperature of 716 °C at 6 kbar and a minimum temperature of 624 °C at 6 kbar. The K_D stability curves are shown in Fig. 10.

The thermometer probably gives somewhat too high temperatures. Rocks of pelitic composition will start to melt at about 650-700 °C if saturated with water (Bucher & Frey 1994). In this study no migmatite formation has been observed either in outcrop or in thin-section. However, the melting temperature is strongly dependent on the aH_2O. As the H_2O pressure decreases, the temperature for incipient partial melting will rise. If the fluid pressure in the rocks is lower than unity, no melting occurs despite the high temperature. On the other hand, in calculating the K_D values, all iron in the biotite is considered to be in the ferrous state. In most cases this is not true, since biotite usually has a certain amount of ferric iron in the tetrahedral position. Using too high a quantity of ferrous iron in the thermometer will give a too high calculated equilibrium temperature. In order to make a reasonable adjustment of the ferric-ferrous ratio in the analysed biotites, published biotite analyses of corresponding metamorphic rocks have been studied. The great majority of biotites have a ferrous content that varies between 85 and 95% (of total iron), with a mean of 90% (see, for instance; Deer et al. 1962, 1992). According to this result, the iron content in the biotites has been recalculated to a fixed ferric-ferrous ratio of 1:9 (i.e. Fe^{3+}/Fe^{2+} = 1:9). In doing so, the K_D curves move to the left in the PT diagram, indicating temperatures of, respectively, 680 °C and 588 °C at 6 kbar. The adjusted K_D curves are shown as broad lines in Fig.10.

If the adjusted K_D min. line (garnet core together with inclusions of biotite in the core area) is combined with reaction 5 in Fig. 9, the position of the intersection point of the two curves falls within the stability field for the two-mineral assemblage alm+ky (Fig 11).The assemblage is diagnostic for the early stages of upper amphibolite facies in the pelitic rocks. Using the position of the intersection point as a quantitative measure of the PT conditions, one obtains a temperature of c. 680 °C and a pressure of 7.5-8.5 kbar (Fig. 11). The lack of staurolite in the matrix of the gneiss also suggests that the temperature is higher than c. 670 °C (see above). It is believed that the temperature and pressure represents the metamorphic conditions during the F_1 folding and the development of the main schistosity, S_1.

The second PT condition represented by K_D values from the garnet-rim together with matrix biotite is harder to define; or expressed in another way, there are no curves that intersect with the K_D line, defining a point or a restricted area in the PT diagram for the temperature and pressure. However, the K_D max. line gives a temperature that is about 100 °C below the maximum temperature obtained from the K_D min. line (Fig. 10). The K_D max. method is supposed to give information about the lowest

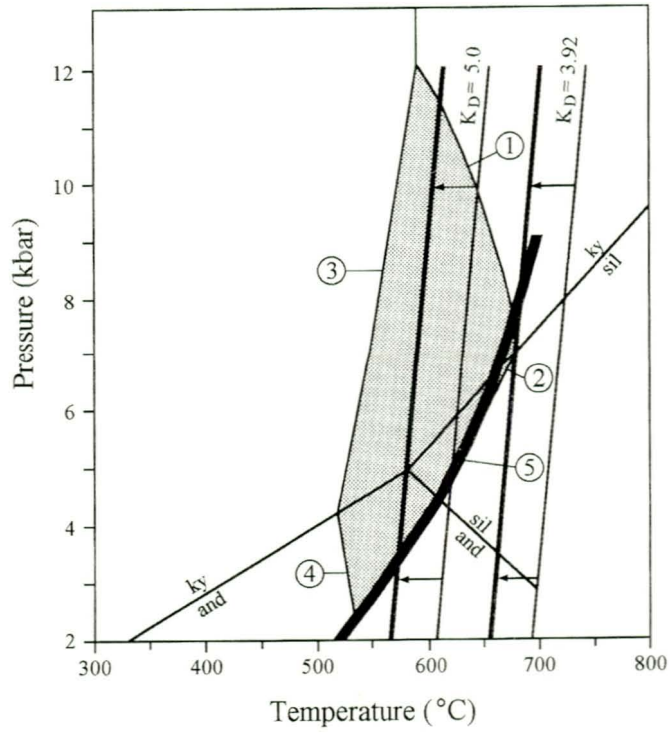

Fig. 11. Combination of the information given in Figs. 9 and 10. See text for further explanation.

equilibrium temperature for the coexisting minerals. As most of the garnet rim - matrix biotite analyses actually give temperatures that are around 100 °C lower than the maximum, it is reasonable to assume that this must have a geological significance. It is interesting to note that the estimated second temperature is in good agreement with temperatures given by Cook (1993) from the Bleikvassli mine area, c.10 km farther south. Using the garnet-biotite calibration of Perchuk & Lavrent'eva (1983) on coexisting garnet (rim composition)-biotite pairs and the garnet-staurolite calibration of Hutcheon (1979) on coexisting garnet-staurolite pairs, he obtained mean temperatures of, respectively, 562±31 and 580±5°C at 8 kbar. Another study from the same area give peak metamorphic conditions of 540-570°C at 7.5-7.9 kbar (Rosenberg et al. 1996). The estimation is based on a variety of silicate and sulphide geothermometers and geobarometers. It is not specified which silicate thermometers were used or whether the studies were carried out on rims or cores.

The studies in the Bleikvassli area clearly demonstrate the importance of a metamorphic equilibrium temperature at around 570-580°C. However, as the somewhat higher maximum PT condition (680°C and 7.5-8.5 kbar) in the Brygfjell-Simafjell area is thought to represent the metamorphic peak during the F_1 folding, the second equilibrium temperature must represent a later event, at least in that area. Thin-section studies of the textural relationships between the minerals indicate that the growth of the idioblastic rim of the garnet is probably restricted to pre- and/or syn- the formation of the F_2 folds, while the formation of the retrograde mineral assemblage has taken place after the two main (F_1, F_2) episodes, presumably under post-peak conditions. It is therefore most reasonable to relate the second equilibrium temperature to the formation of the F_2 folds. In that case a drop in the temperature of 100°C must have taken place between the two main episodes. However, since penetrative structural elements such as schistosity, etc., in association with the F_2 folding are mostly lacking, it has not been possible to establish an unambiguous correlation between the temperature and the fold episode. The conclusion regarding the geological relationships is therefore saddled with some uncertainties.

Conclusions

(1) Two tectonostratigraphic units can be distinguished in the studied area. The upper unit, the Brygfjell Group, is composed mainly of marbles, garnet-mica schists and amphibolites, whereas the underlying Bjørnskolten Group is largely made up of a variety of gneisses (garnet-mica gneiss, garnet-kyanite-muscovite gneiss, feldspar-mica gneiss, mica gneiss, quartzitic gneiss and granitic gneiss).

(2) The rocks have been affected by four clearly distinguishable phases of folding. The first two phases (F_1 and F_2) led to the development of tight to isoclinal folds, whereas the last two (F_3, F_4) produced open folds. The regional schistosity, S_1, is associated with the first phase of folding, while the most prominent mineral lineation, including extended feldspar augen, belongs to the F_2 phase. In appropriate rocks a second schistosity (S_2) may be seen in association with the F_2 folding although the structure is usually poorly developed.

(3) It is possible to separate two main stages of mineral growth. The main assemblage (M_1) defines the S_1 foliation and the principal growth period was during the F_1 deformation. The minerals belonging to the M_1 association are folded around microscopic F_2 folds and with small modifications (some minerals, especially garnet, occur with a zonation where the outermost rims cut the foliation) were also stable under the F_2 deformation. Except for the (local) mineral lineation and the sporadic presence of white mica parallel to the axial planes of the F_2 folds, there is no specific mineral growth related to the F_2 deformation. However, the garnet rims are considered to have grown over a period of time from post-F_1 to syn- F_2.

(4) The second or retrograde mineral association (M_2) is represented by chloritisation of garnet, biotite and amphibole in appropriate rocks and a sericitisation/saussuritisation of plagioclase and Al-silicates. A randomly distributed muscovite also probably belongs to the retrograde assemblage. It is not possible to relate the secondary minerals to any specific structural elements. However, the textural relationships indicate that the replacement processes have taken place over a long period of time, probably representing various stages of alteration during uplift and cooling in the Caledonian orogenic belt.

(5) The metamorphic peak occurred during the first phase of folding and is estimated to 680°C and 7.5-8.5 kbar. The PT estimate is based on different types of mineral reactions (reaction isograds) and index minerals in combination with garnet-biotite equilibrium temperatures, calculated by use of geothermometry. The highest garnet-biotite temperatures, which are also in good agreement with the temperature interval for the mineral reactions, are derived from garnet cores and inclusions of biotite in the core areas. Calculations using garnet rims together with matrix biotite yield temperatures which are about 100 °C lower than the maximum. It is suggested that this could represent the closing temperature conditions during the F_2 folding.

Acknowledgements

The author is grateful to Stephen Lippard for his critical reading of the first draft of the manuscript while Magne Gustavson and Per-Gunnar Andréasson are thanked for constructive criticism and comments at the reviewing stage. David Roberts has kindly improved the English and

Anne-I Johannessen drafted the illustrations. The fieldwork was financed by the Geological Survey of Norway (NGU) while the analytical work was supported by The Norwegian Institute of Technology, University of Trondheim. To these persons and institutions I offer my sincere thanks.

References

Brattli, B., Tørudbakken, B.O. & Ramberg, I.B. 1982: Resetting of a Rb-Sr total rock system in Rödingsfjället Nappe Complex, Nordland, North Norway. *Nor. Geol. Tidsskr. 62*, 219-224.

Brattli, B. & Tørudbakken, B. 1987: Arsdaddalen. Description of the geological map ASM-M711, 2028 IV, scale 1: 50 000. *Nor. geol. unders. Skrifter 81*, 1-39.

Bhattacharya, A. Mohanty, L. Maji, A. Sen, S.K. & Raith, M. 1992: Non-ideal mixing in the phlogopite-annite binary: constraints from experimental data on Mg-Fe partitoning and reformulation of the biotite-garnet geotermometer. *Contrib. Mineral. Petrol. 111*, 87-93.

Bucher, K. & Frey, F. 1994: *Petrogenesis of metamorphic rocks (6th. ed).* Springer-Verlag. Berlin, Heidelberg, New York, 318 pp.

Claesson, S. 1979: Pre-Silurian orogenic deformation in the north-sentral Scandinavian Caledonides. *Geol. Fören. Stockh. Forh. 101*, 353-356.

Cribb, J.S. 1981: Rb-Sr geochronological evidence suggesting a reinterpretation of part of the north Norwegian Caledonides. *Nor. Geol. Tidsskr. 61*, 97-110.

Cook, N.J. 1993: Condition of metamorphism estimated from alteration lithologies and ore at the Bleikvassli Zn-Pb- (Cu) deposit, Nordland, Norway. *Nor. Geol. Tidsskr. 73*, 226-233.

Deer, W.A., Howie, R.A. & Zussman, J. 1962: *Rock-forming minerals. Vol 3, Sheet silicates.* Longmans, London, 270 pp.

Deer, W.A., Howie, R.A. & Zussman, J. 1992: *An introduction to rock-forming minerals. (2nd. ed).* Longman Scientific & Technical, Essex, 696 pp.

Eggert, R.G. & Kerrick, D.M. 1981: Metamorphic equlibria in the siliceous dolomite system: 6 kbar experimental data and geologic implications. *Geochim. Cosmochim. Acta 45*, 1039-1049.

Eggleton, R.A. & Banfield, J.F. 1985: The alteration of granitic biotite to chlorite. *Am. Min., 70*, 902-910.

Ferry, J.M. & Spear, F.H. 1978: Experimental calibration of the partitoning of Fe and Mg between biotite and garnet. *Contrib. Mineral. Petrol. 66*, 113-117.

Gjelle, S. 1978: Geology and structure of the Bjøllånes area, Rana, Nordland. *Nor. geol. unders. 343*, 1-37.

Gustavson, M. 1975: The low - grade rocks of the Skålvær area, S. Helgeland and the relationship to the high - grade rocks of the Helgeland Nappe Complex. *Nor. geol. unders. 322*, 13-33.

Gustavson, M. 1978: Caledonides of North-Central Norway. *Geol. Surv. Canada, Pap. 78-13*, 25-30.

Gustavson, M. 1982: Geologisk kart over Norge. Berggrunnskart Mosjøen - M 1: 250 000. *Nor. geol. unders.*

Gustavson , M., Brattli, B., Seir Hansen, T. & Søvegjarto, U. 1990: Korgen berggrunnskart 1927 2, 1:50 000, foreløpig utgave. *Nor. geol. unders.*

Gustavson, M. & Gjelle, S. 1991: Regional geology of central Nordland. *Earth Evol. Sci. 1*, 6-13.

Gustavson, M. & Gjelle, S. 1992: Geologisk kart over Norge. Berggrunnskart Mo i Rana - M 1: 250 000. *Nor. geol. unders.*

Hutcheon, I. 1979: Sulfide-oxide-silicate equilibria, Snow Lake, Manitoba. *Amer. Jour. Sci. 279*, 643-665.

Kulling, O. 1955: Beskrivning till berggrunnskarta över Västerbotten län. 2. Den Kaledonske fjällkjedjans berggrund inom Västerbotten län. *Sver. Geol. Unders., Ser. Ca. 37*, 101-296.

Perchuk, L.L. & Lavrent'eva, J.V. 1983: Experimental investigation of exchange equilibria in the system cordierite-garnet-biotite. In Saxena, S.K. (ed.): *Kinetics and Equilibria in Mineral Reactions*, Springer Verlag, 119-239

Ramberg, I.B. 1967: Kongsfjellområdets geologi - en petrografisk og strukturell undersøkelse i Helgeland, Nord-Norge. *Nor. geol. unders. 240*, 152 pp.

Ramberg, I.B., & Stephens, M.B. 1981: The Central Scandinavian Caledonides - Storuman to Mo i Rana. Uppsala Caledonide Symposium. Excursion A3. Excursion guide.

Ramsay, J.G. 1967: *Folding and fracturing of rocks.* McGraw-Hill Book Company, New York, 568 pp.

Riis, F. & Ramberg, I.B. 1979: Nyere data fra Nordlands høymetamorfe dekkekompleks. (Abstract). *Geolognytt 13*, 60-61.

Rosenberg, J.L., Spry, P.G., Jacobsen, C.E. & Vokes, F.M. 1996: The effects of sulfidation and oxidation on the composition of biotite and garnet associated with the Bleikvassli Zn-Pb-(Cu) deposit Nordland, Norway: A preliminary study. *GSA, North-central section meeting, May 1996, Books of abstract (in press).*

Rutland, R.W.R. 1959: Structural geology of the Sokumvatn area, North Norway. *Nor. Geol. Tidsskr. 39*, 287-337.

Rutland, R.W. R. & Nicholson, R. 1965: Tectonics of the Caledonides in part of Nordland, Norway. *Q. J. Geol. Soc. Lond. 121*, 73-109.

Skauli, H., Bjørlykke, A. & Thorpe, R.I. 1992: Lead-isotope study of the sulphide ore and alteration zone, Bleikvassli zinc-lead deposit, northern Norway. *Mineral. Deposita 27*, 276-283.

Spear, F.S. 1993: *Metamorphic phase equlibria and pressure-temperature-time paths.* Mineralogical Society of America Monograph. Washington, D.C., 799 pp.

Stephens, M.B., Gustavson, M., Ramberg, I.B., & Zachrisson, E. 1985: Caledonides of the central-north Scandinavia - a tectonostratigraphic overview. *In* Gee, D.G. & Sturt, B. A. (eds): *The Caledonide Orogen - Scandinavia and Related Areas.* John Wiley & Sons Ltd., Chichester, 135-162.

Tørudbakken, B.O. & Brattli, B. 1985: Ages of metamorphic and deformational enents in the Beiarn Nappe Complex, Nordland, Norway. *Nor. geol. unders. Bull. 399*, 27-39.

Winkler, H.G.F. 1979: *Petrogenesis of Metamorphic Rocks (5th.ed.).* Springer - Verlag, New York, Heidelberg, Berlin, 348 pp

Manuscript received June 1995, revised manuscript accepted February 1996